J Wood Sci (2006) 52:483–489
DOI 10.1007/s10086-005-0795-7

ORIGINAL ARTICLE

Kosei Ando · Yoshihiko Hirashima · Mina Sugihara
Sakiko Hirao · Yasutoshi Sasaki

Microscopic processes of shearing fracture of old wood, examined using the acoustic emission technique

Received: April 11, 2005 / Accepted: December 21, 2005 / Published online: April 25, 2006

Abstract We examined the process of microscopic fracturing peculiar to old wood, based on the generation characteristics of acoustic emission (AE) events and fracture surface analysis. The shearing tests of old wood obtained from construction-derived lumber and new wood within 3 years after lumbering were performed in accordance with the Japanese Industrial Standards (JIS Z 2101-1994). The species of wood used in this study was Japanese red pine. The old wood had been used as a beam in a building for 270 years. The number of the occurrences of AEs at low load levels was larger in the old wood than in the new wood. As a result of analyzing the AE amplitude distributions, we found that the period in which AEs with small amplitudes were frequently generated was longer in the old wood than in the new wood. Also, the fracture surfaces after the final rupture under scanning electron microscope showed more uneven and complicated surfaces in the old wood. Based on the above findings, we presume that during the shearing test the old wood underwent a relatively long and stable progress of microcracking before the final fracture.

Key words Old wood · Reuse · Acoustic emission · *m*-Value · Fractography

Introduction

Wood has long been called an ecomaterial. In making a green sustainable society a reality, it is quite important to establish reuse or recycling systems for wood. However, in spite of the fact that wood has the potential of being an ecomaterial, we cannot really say that wood is used effectively today. In Japan, as much as 5 million tons of construction-derived woods (hereinafter referred to as old wood) are generated every year.[1] The resource recovery rates for construction debris in 2002 were high, 99% and 98%, for asphalt concrete and concrete, respectively, and low, 61%, for old wood.[2] The reconstitution of wood through the agglomeration of wood chips into boards, etc., that is, the recycling of wood, accounts for most of the wood recovery mentioned here. While such reconstitution is effective in terms of the recycling of resources, the burden on the environment caused by the energy required for this type of processing should be taken into consideration.

What we have an interest in is not the aforementioned recycling of old wood, but its reuse, that is, the use of old wood as it is or with minimum processing or treatment, because such reuse will place little burden on the environment as far as processing or treatment is concerned, and it enables the most efficient utilization of resources. However, so far there have not been many cases of reuse of old wood. Cases of reuse are frequently limited to reuse of the wood as nonconstruction materials, such as ornaments. The main reason for this is that the strength characteristics of old wood remain unclear in many respects; another reason is that there are problems related to the current social system, especially regarding distribution and legal standards. Although Japan has many wooden buildings with a long, proud tradition and enjoys the culture of wood, in many cases in which these buildings were repaired, the old wooden elements were replaced by new wooden elements because the serviceability of the existing old elements could not be determined due to the lack of proper technology to evaluate their strength performance. As just described, even when it is imperative to maintain the authenticity of traditional architectural structures so that they can be handed down to posterity, under the present circumstances, problems remain in the reuse of old wood.

In previous reports,[3–5] the strength characteristics of new and old woods were compared using the technique of compensating the difference in density distribution between new and old woods (Monte Carlo simulation) for the purpose of examining the strength characteristics of old wood,

K. Ando (✉) · Y. Hirashima · M. Sugihara · S. Hirao · Y. Sasaki
Graduate School of Bioagricultural Sciences, Nagoya University, Chikusa-ku, Nagoya 464-8601, Japan
Tel. +81-52-789-4149; Fax +81-52-789-4147
e-mail: musica@agr.nagoya-u.ac.jp

in view of reusing it as constructional material. This technique had not been taken into consideration in the studies theretofore. The comparison has revealed, for instance, that the tensile strength was lower in old wood, whereas the compressive strength of the old Japanese red pine was higher than that of new wood of the same species.

The environment in which old wood is used as a constructional material is not always limited to a static mechanical environment. Old wood can also be subjected to creep or fatigue, due to repetitive loading. Changes in temperature and humidity should be assumed. Changes in the strength characteristics under such various loading conditions should also be considered. Therefore, it is essential to know the internal structural changes of the deformed old wood, and to understand the characteristics of the fractures, which are presumed to be different from those of new wood. As a technique of quantifying the internal structural change under loading in real time, the acoustic emission (AE) method has been found to be effective. In wood, AE is produced in close relation with the beginning and development of cracks.[6,7] Ando et al.[8] have estimated the differences in the deformation and fracture mechanisms between woods with different grain angles using a combination of the AE method and fractography.

This study examined the process of microscopic fracturing, which seems to be peculiar to old wood, by comparing the AE characteristics and the fracture surface observed under a scanning electron microscope (SEM), with the aim of understanding the deformation and fracture characteristics of old wood.

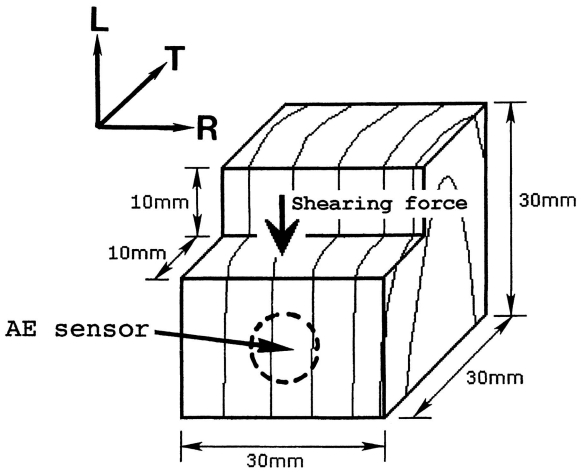

Fig. 1. Shearing test specimen. Shearing surface is an LR plane

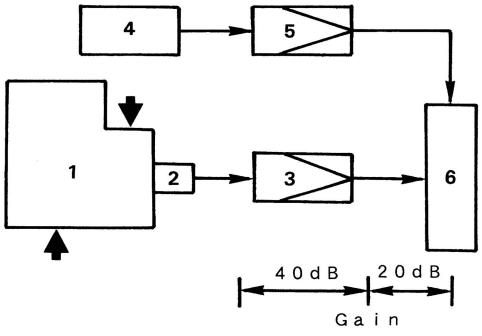

Fig. 2. A block diagram of the acoustic emission (AE) measuring system. *1*, Test specimen; *2*, AE sensor; *3*, preamplifier; *4*, load cell; *5*, strain amplifier; *6*, AE measurement equipment (SAE-1000A)

Materials and methods

Specimens

The species of wood used in this study was Japanese red pine (*Pinus densiflora* Sieb. et Zucc.). The old wood used in the test had been used for 270 years as a beam in the main building of a Buddhist temple in Nagano Prefecture in Japan. The new wood used for comparison purposes was also produced in Nagano Prefecture and had been lumbered within the 3 years before the testing. The specimen was a chair-type shearing specimen conforming to the Japanese Industrial Standards (JIS Z2101-1994), as shown in Fig. 1.

Experimental method

The shearing tests were performed in accordance with Japanese Industrial Standards (JIS Z 2101-1994) using an Instron-type testing machine (Autograph AG-10; Shimadzu). A crosshead speed of 0.6 mm/min was applied to the specimens.

The AE monitoring was made simultaneously with the shearing tests using AE measurement equipment (SAE-1000A; Shimadzu). Figure 2 illustrates a block diagram of the AE measuring system. AE signals, detected by a piezoelectric transducer with a resonant frequency of 200 kHz (S-20DSA; Shimadzu), were submitted to a bandpass filter (100–500 kHz) and amplified by a preamplifier and main amplifier. The total amplification level of the system was maintained at 60 dB. The threshold value (38 mV) was set to the minimum noise-free level. AE monitoring was continued until the load attained its maximum value. The fracture surfaces were observed using a SEM (S-4500; Hitachi) after the tests.

The microfibril angle in the S2 layer of each specimen was measured by the improved Cave's method[9] using an X-ray diffractometer (XD-D1w; Shimadzu). The crystallinity of wood was also measured from the X-ray diffraction patterns of wood powders. The tube was operated at 35 kV and 35 mA. The wood powders were stacked on a sample holder and scanned from 40 to 5 degrees. The diffracted intensity (in counts) was measured as a function of 2θ. Relative crystallinity (degree of crystallization) of wood was estimated using the following equation:[10]

$$\text{Crystallinity}(\%) = \frac{I_c}{I_a + I_c} \times 100 \quad (1)$$

where I_a is the amorphous area on the X-ray diffractogram and I_c is the crystallized area on the diffractogram.

Table 1. Density, moisture content, ultimate shearing strength (τ_{TL}), width of annual ring, and percentage of latewood of Japanese red pine

Test specimen	Density (kg/m^3)	MC (%)	τ_{TL} (MPa)	WA (mm)	PL (%)	*n*
New wood	486 (15)	10.7 (0.2)	12.4 (1.1)	3.88 (1.56)	21.9 (8.4)	16
Old wood	472 (22)	10.6 (0.1)	11.3 (2.1)	4.07 (1.38)	20.2 (6.5)	16

Numbers in parentheses are standard deviations
MC, moisture content; WA, width of annual ring; PL, percentage of latewood

Results and discussion

Structural parameters and ultimate shearing strength

Table 1 shows the density, moisture content, ultimate shearing strength (τ_{TL}), width of annual ring, and percentage of latewood of the new and old woods. The *t*-tests showed no difference between the new and the old woods in these parameters, at a significance level of 5%. Also, as a result of Monte Carlo simulation to adjust the distribution shape of density of new wood to that of the old wood, no significant difference in shearing strength was observed between the woods.[4]

Table 2 shows the microfibril angle in the S2 layer and the crystallinity of wood. There was no statistical difference between the new and old woods in these parameters, at a significance level of 5%. Kohara and Okamoto[11] studied the permanence of old timber and reported that the crystallinity of wood increases with time within 350 years after building. This understanding was different from the results of Table 2.

Table 2. Microfibril angle in the S2 layer and crystallinity of Japanese red pine

Test specimen	Microfibril angle (degrees)	Crystallinity (%)
New wood	16.3 (3.6)	35.3 (0.6)
Old wood	14.6 (1.7)	34.9 (1.6)

Numbers in parentheses are standard deviations

Characteristics of AE

Progression of cumulative AE event count

Figure 3 shows the changes in the total number of AE events up to the maximum stress. For the new wood, the period in which the frequency of the occurrence of AE events was low continued for a long while after the first occurrence, but the AE events tended to increase in number abruptly just before the final fracture. For the old wood, the period in which the frequency of the occurrence was high continued from the first occurrence up to the final fracture. It is remarkable that a great difference in the cumulative AE event count was observed between the new and the old woods, especially at the initial stage of loading.

Table 3 shows the stress at the first occurrence of an AE event, the cumulative AE event count at 30% of maximum stress, and the number of occurrences up to the maximum stress. The *t*-tests showed, at the significance level of 0.1%, that the stress at the first occurrence was smaller in the old wood and that the cumulative AE event count at 30% of maximum stress was larger in the old wood. The AEs were generated by the microscopic fracturing of the material. Accordingly, it seems that in the old wood the microscopic fractures occurred at an earlier stage of loading on comparison with the new wood, and the fractures grew gradually. The old wood used in this study had been used as a beam in an architectural structure for as long as 270 years. During that period, the old wood must have undergone fluctuations in humidity and temperature between day and night or between seasons, various climatic conditions such as snows and storms, and several earthquakes. The authors suppose that, under such conditions, numerous minuscule cracks had been produced that did not affect its strength, and that the AE events were generated from such minuscule cracks under low-load conditions.

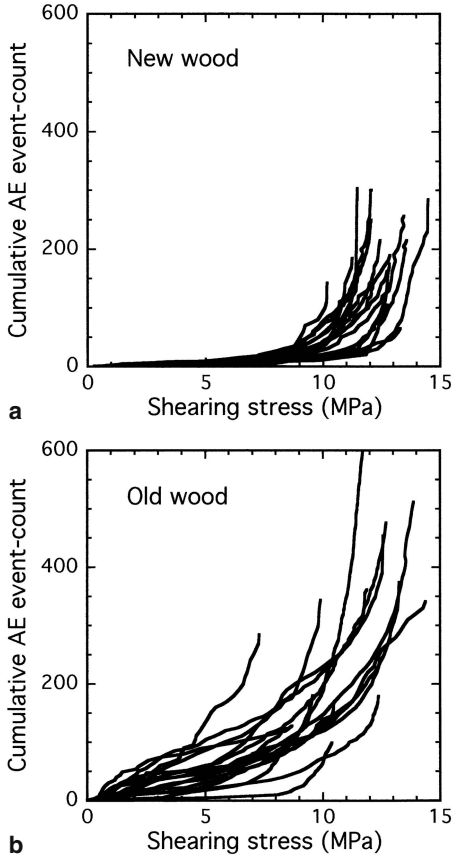

Fig. 3. Progression of cumulative AE event counts up to the maximum stress for **a** new wood and **b** old wood

Table 3. Stress at first acoustic emission (AE) count, cumulative AE event count at 30% of maximum stress, and cumulative AE event count at maximum stress

Test specimen	Stress at first AE count (MPa)	Cumulative AE event count at 30% of maximum stress	Cumulative AE event count at maximum stress
New wood	2.01 (1.38)*	4.5 (2.2)*	210.3 (69.3)
Old wood	0.31 (0.25)*	38.4 (21.2)*	304.6 (153.1)

Numbers in parentheses are standard deviations
*$P < 0.001$; *t*-test between new and old woods

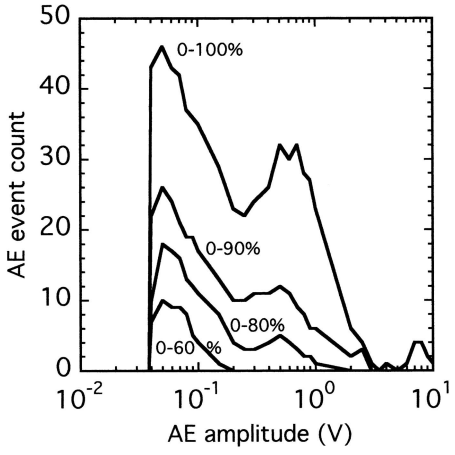

Fig. 4. Examples of AE amplitude distribution up to the maximum stress. Percentages represent the ratios of the stress to the maximum stress

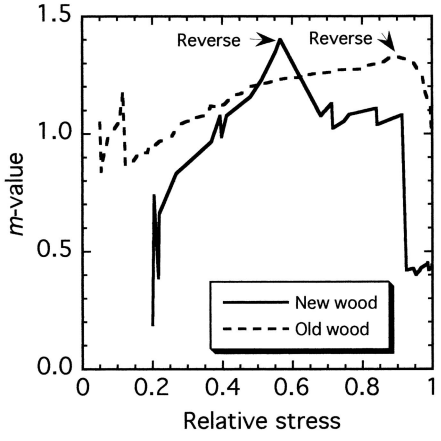

Fig. 5. Typical progression of *m*-values. Relative stress is defined by the ratio of the stress to the maximum stress

Progression of m-value

It is thought that, if the situations at the source of AE can be determined, this information would be the key to elucidating the complex microscopic fracturing mechanism of the wood. One indicator of the magnitude of an AE wave is the maximum amplitude of the AE signal. An AE amplitude distribution map, with the maximum amplitude value along the horizontal axis and the number of occurrences along the vertical axis, is considered to indicate the AE energy distribution. Figure 4 shows examples of AE amplitude distribution. At the initial stage, only AE events with small amplitudes, with a peak of 50 mV, occurred, but AE events with large amplitudes, a peak of 500 mV, began to occur gradually. The fact that at the beginning only AE events with small amplitudes occurred and that those events with large amplitudes began to occur gradually suggests a gradual increase in the scale of the microscopic fractures. Also, the existence of two amplitude peaks suggests the existence of two fracture sources with different released energies.

In general, the following relational expression holds between the number of AE events and the maximum amplitude value for each AE wave:[12,13]

$$N(V) = kV^{-m} \tag{2}$$

where V is the peak amplitude of each AE wave, $N(V)$ is the number of AE waves having the amplitude V, and k and m are constants. When both sides in Eq. 2 are processed with a common logarithm:

$$\log N(V) = \log k - m \log V \tag{3}$$

Equation 3 is an empirical rule; that is, the Ishimoto-Iida equation from the field of seismology was applied to the study of AEs. It is known that the *m*-value can be an effective AE parameter, because it conforms to the quality of the materials and the state of the progress of deterioration and cracking. To evaluate the AE amplitude distributions quantitatively, the progression of the *m*-value is discussed in this study. Figure 5 shows typical examples of change in the *m*-value. In both the new wood and the old wood, the *m*-value fluctuated greatly immediately after the beginning of loading, and increased thereafter. Upon reaching a certain load, the value began to decrease until the final fracture. Some specimens of the old wood underwent the final fracture with the *m*-value still high instead of having decreased. The increase in the *m*-value signifies the frequent occurrence of small-amplitude AEs, and the decrease in the *m*-value signifies the frequent occurrence of high-amplitude AEs. With this evaluation method of *m*-value as a basis, we hypothesized the situations at the source of AE as follows.

The developmental stages of the fracturing of wood can be understood as comprising the initiation of cracks, the stable propagation of cracks, and the unstable fractures.[14,15] At the stage of stable propagation, fractures with relatively small released energies, such as the single-cell-level delamination, split, cutting, and exfoliation at the interface with

contiguous cells are expected. On the other hand, regarding the unstable fractures, because fractures such as cutting or exfoliation are expected to occur in tens or hundreds of cells within a short time, the released energy is expected to be great. Accordingly, it is presumable that the stage at which the *m*-value increases corresponds to the stage with predominantly stable propagation of cracks, whereas the stage at which the *m*-value decreases corresponds to the stage with predominantly unstable fractures.

Figure 6 shows the quantitative difference in the progression of *m*-value between new wood and old wood, considering that the point at which the *m*-value shifts from an increase to a decrease is an indicator of the change from stable propagation to unstable fracturing. The vertical axis represents the ratio of the stress range in which the *m*-value increases to the maximum stress. It was found that the stress range with *m*-value increase was greater in the old wood. Also, the *t*-test showed a difference between the new and old woods at a significance level of 0.1%. That is, it could be concluded based on the generation behavior of the AEs that the period of stable propagation of cracks was longer in the old wood than that in the new one.

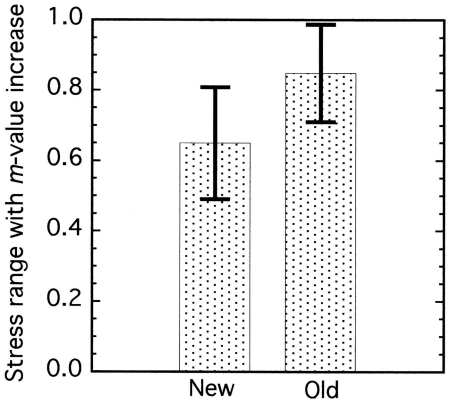

Fig. 6. The difference in the stress range in which the *m*-value increases between new and old woods. The vertical axis is the ratio of the range to the maximum stress. *Error bars* show standard deviations. There is a significant difference (*t*-test) at $P < 0.001$

Fractographical features of microfracture surfaces

As mentioned above, the difference in the process of microscopic fracturing between the new wood and the old wood was estimated based on the progressions of the cumulative AE event count and the *m*-value. Next, the fracture surface, which appeared as a result of the final rupture, was observed and examined under an SEM. Figures 7 and 8 show examples of scanning electron micrographs of typical fracture surfaces. Although it must be acknowledged that the fracture surface of wood is not uniform and that there are various fracture types, Figs. 7 and 8 show fracture surfaces that are considered to be dominant in new wood and old wood, respectively.

The fracture surface of the new wood was flat and smooth (Fig. 7). Regarding the fracture type, an intrawall failure[16] caused by the propagation of cracks along the interfaces between the cells was dominant. On the other hand, the fracture surface of the old wood was rough and irregular (Fig. 8). Regarding the fracture type, a trans-wall failure[16] caused by the propagation of cracks by cutting cell walls, in addition to an intrawall failure, was frequently observed. The old wood showed more complicated fracture modes than the new wood; the reason for this is that the old wood

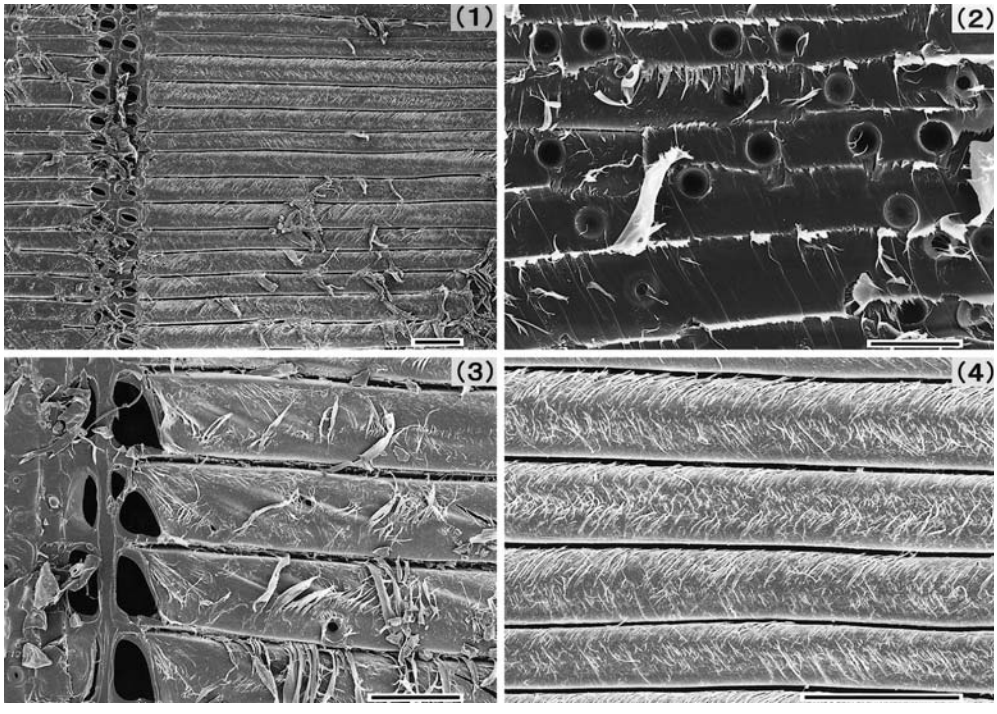

Fig. 7. Examples of intrawall failure, which was dominantly observed in the new wood. *1*, New wood, density = 506 kg/m^3, τ_{TL} = 12.8 MPa, width of annual ring (WA) = 3.33 mm, percentage of latewood (PL) = 25.3%; *2*, new wood, density = 479 kg/m^3, τ_{TL} = 12.1 MPa, WA = 4.25 mm, PL = 20.1%; *3*, new wood, density = 482 kg/m^3, τ_{TL} = 11.5 MPa, WA = 4.88 mm, PL = 19.5%; *4*, new wood, density = 506 kg/m^3, τ_{TL} = 12.8 MPa, WA = 3.33 mm, PL = 25.3%. *Bars* 50 μm

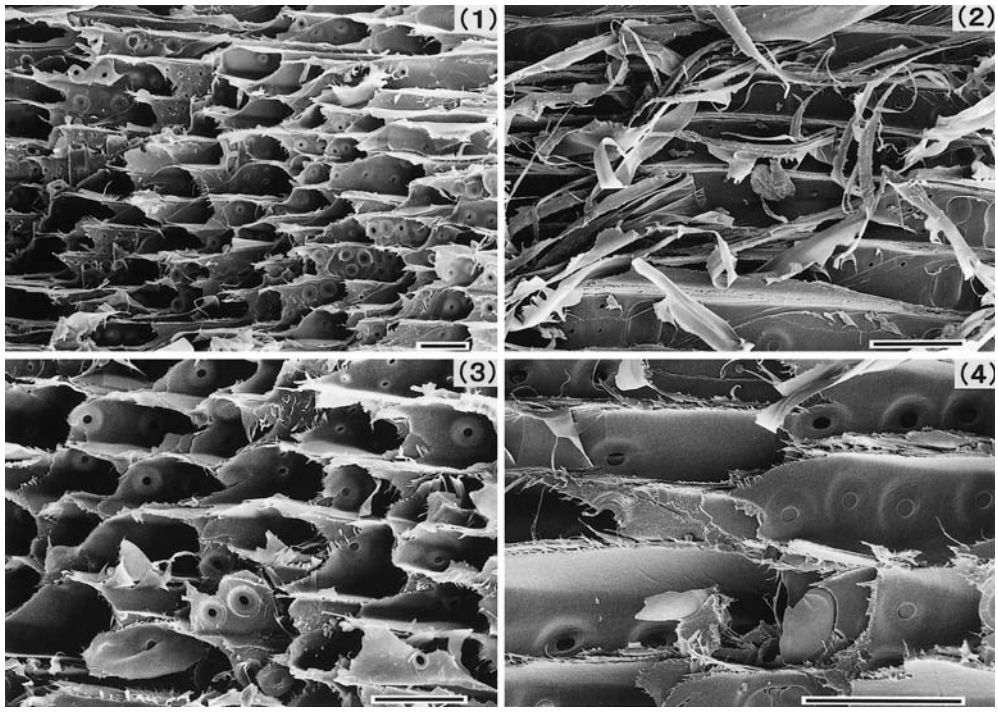

Fig. 8. Examples of the trans-wall failure, which was dominantly observed in the old wood. *1*, Old wood, density = 494 kg/m^3, τ_{TL} = 13.3 MPa, WA = 3.22 mm, PL = 20.7%; *2*, old wood, density = 474 kg/m^3, τ_{TL} = 11.9 MPa, WA = 4.38 mm, PL = 23.7%; *3*, old wood, density = 494 kg/m^3, τ_{TL} = 13.3 MPa, WA = 3.22 mm, PL = 20.7%; *4*, old wood, density = 486 kg/m^3, τ_{TL} = 9.6 MPa, WA = 4.27 mm, PL = 18.8%. *Bars* 50 μm

passed through various stages of fracture before the final fracture.

In the old wood we observed that many trans-wall failures were initiated from the bordered pits (Fig. 8). The pit plays an important role in concentrating stress. Accordingly we consider that the microcracks, which occurred over a period of 270 years, had already existed at the pit borders.

Estimation of the microfracture processes by AE technique

Based on the above results of the AE measurement and the fracture surface analysis, the difference in the development of microscopic fractures between the new wood and the old wood was examined. Regarding the old wood, stress at the first occurrence of an AE event was small, and subsequent AE events frequently occurred under low load. Also, the period of the increase in the *m*-value, which was assumed to coincide with the period of stable propagation of cracks, was long. Accordingly, we think that the period in which cracks were initiated and developed in a stable manner continued for a relatively long time before the final fracture. As a result, it seems that the rough, irregular, and complex fracture surface with mixed and combined fracture types dominantly appeared. Regarding the new wood, stress at the first occurrence of an AE event was great, and subsequent AE events occurred infrequently under low load. Also, the period of the increase in the *m*-value was short. Accordingly, we think that the period of stable propagation was relatively short before the final fracture. The surface of the fracture, which is presumed to have occurred through this process, was flat and smooth.

The microcracks that occurred through stable propagation affected the strength of the material. While weakening due to cracks is easily imaginable, an increase in the strength due to the redistribution of stress can also be presumed.[17,18] Perhaps it would have a significant effect on the strength characteristics of the old wood whether the cracks that developed from microscopic cracks over a period of 270 years have had a bad or a good effect.

Conclusions

The difference in the shearing fracture mode between the Japanese red pine that had been used for 270 years as a beam in a Buddhist temple and new Japanese red pine within 3 years after lumbering was estimated based on the generation characteristics of AE events and the fracture surface analysis. The results suggest that the old wood underwent the final fracture after a relatively long period of stable propagation of cracks, whereas the new wood underwent the final fracture with almost no previous period of stable propagation.

It is unclear whether such differences in the fracture mode apply to other types of loading (tension, bending, and compression); this remains a future subject of examination.

References

1. Ministry of Land, Infrastructure, and Transport of Japan (2003) 2002 survey on the state of construction byproducts (in Japanese). Tokyo, pp 1–9

2. Ministry of Land, Infrastructure, and Transport of Japan (2005) Creating and conserving a beautiful and favorable environment. In: White paper on land, infrastructure, and transport in Japan, 2004. Tokyo, pp 61–65
3. Hirashima Y, Sugihara M, Sasaki Y, Ando K, Yamasaki M (2004) Strength properties of aged wood I: tensile strength properties of aged keyaki and akamatsu woods (in Japanese). Mokuzai Gakkaishi 50:301–309
4. Hirashima Y, Sugihara M, Sasaki Y, Ando K, Yamasaki M (2004) Strength properties of aged wood II: compressive strength properties, shearing strength and hardness of aged keyaki and akamatsu woods (in Japanese). Mokuzai Gakkaishi 50:368–375
5. Hirashima Y, Sugihara M, Sasaki Y, Ando K, Yamasaki M (2005) Strength properties of aged wood III: static and impact bending strength properties of aged keyaki and akamatsu woods (in Japanese). Mokuzai Gakkaishi 51:146–152
6. Ansell MP (1982) Acoustic emission from softwoods in tension. Wood Sci Technol 16:35–59
7. Ando K, Sato K (1993) Direct observation of micro-fracture process of wood by SEM and its acoustic emission characteristics under tension test (in Japanese). In: Proceedings of the 1993 national conference on acoustic emission, Okinawa, pp 85–90
8. Ando K, Sato K, Fushitani M (1992) Fracture toughness and acoustic emission characteristics of wood II: effect of grain angle (in Japanese). Mokuzai Gakkaishi 38:342–349
9. Yamamoto H, Okuyama T, Yoshida M (1993) Method of determining the mean microfibril angle of wood over a wide range by the improved Cave's method. Mokuzai Gakkaishi 39:375–381
10. Hermans PH, Weidinger A (1948) Quantitative X-ray investigations on the crystallinity of cellulose fibres. A background analysis. J Appl Phys 19:491–506
11. Kohara J, Okamoto H (1955) Studies on the permanence of wood XI: the crystallized region of cellulose in old timbers (in Japanese). J Jpn For Res 37:392–395
12. Nakasa H (1978) Acoustic emission amplitude distribution and its signal processing (in Japanese). J Nondestruct Inspect Jpn 27:236–244
13. Ando K, Ohta M (1995) Relationships between the morphology of micro-fractures of wood and the acoustic emission characteristics. Mokuzai Gakkaishi 41:640–646
14. Debaise GR, Porter AW, Pentoney RE (1966) Morphology and mechanics of wood fracture. Mater Res Stand 6:493–499
15. Furukawa I (1978) Optical microscopic studies on the longitudinal tension failure of notched microtome sections (in Japanese). Mokuzai Gakkaishi 24:598–604
16. Saiki H (1988) Failure modes of wood – basic types and terminology – (in Japanese). J Soc Mater Sci Jpn 37:529–534
17. Gordon JE, Jeronimidis G (1974) Work of fracture of natural cellulose. Nature 252:116
18. Schniewind AP, Bartels HJ, Gammon BW (1979) Effect of preloading on fracture toughness of wood. In: Proceedings of the First International Conference on Wood Fracture, Banff, pp 227–239